Metallocalixarene catalysts: α-olefin polymerisation and ROP of cyclic esters

Carl Redshaw[a,b]

[a] *College of Chemistry and Materials Science, Northwest University, Xi'an, 710069, China.*

[b] *Department of Chemistry, University of Hull, Hull, HU6 7RX, UK.*

Abstract: This perspective review discusses metallocalix[*n*]arene complexes that have been employed in either α-olefin polymerization or in the ring opening polymerization (ROP) of cyclic esters over the last 5 years. Synthesis, molecular structure and catalytic potential are discussed. For α-olefin polymerization, systems based on early transition metals in combination with calix[*n*]arenes (n = 4, 6 or 8), depleted calix[4]arenes or thia/sulfinyl/sulfonyl calix[4]arenes have been reported, and in some cases, are highly active. For the ROP studies, a number of the systems, typically of the early transition metals, only exhibit activity under robust conditions, whereas other systems, for example those of magnesium, demonstrate exceptional activity, immortal behaviour and intriguing stereoselectivity.

Introduction: The family of compounds called calixarenes are so named because of their shape, deriving their name from the Greek word *calix* meaning vase. Depending on the chemical make-up, the cone-like shape makes them well adapted to a range of applications – from possible drugs for the treatment of cancer to frameworks that have large accessible pores and cavities available for gas storage. [1] The larger calix[*n*]arenes (n >4) are more flexible which can be an advantage in terms of accommodating metals bearing bulky substituents. [2] Our interest in metallocalix[*n*]arenes stems from their potential use in catalysis. [3] In particular, we have focussed on the use of early transition metal systems for α-olefin polymerization, studies which have met with mixed success. On the negative side, despite the elucidation of many esoteric

structures based on metals such as niobium, tantalum or chromium, observed catalytic activities were poor. [4] On a more positive note, a number of highly active vanadium-based calixarenes were identified, most notably by changing the calixarene bridging group from a methylene to a dimethyleneoxa group. [5] The use of calixarenes in metal-based catalysis was reviewed by us back in 2008, [3] and since that time we and others have continued to probe the use of metallocalix[*n*]arenes for both α-olefin homo- and co-polymerization and in the ring opening polymerization (ROP) of cyclic esters, typically ε-caprolactone and lactide (eg. See Figure 1). [6] Some of the many attributes that calixarenes possess and the benefits they can impart on catalysis are listed in Table 1. Herein, we discuss some of the recent advances in these areas from our group and others. We note that the coordination chemistry of calixarenes has been reviewed recently. [7]

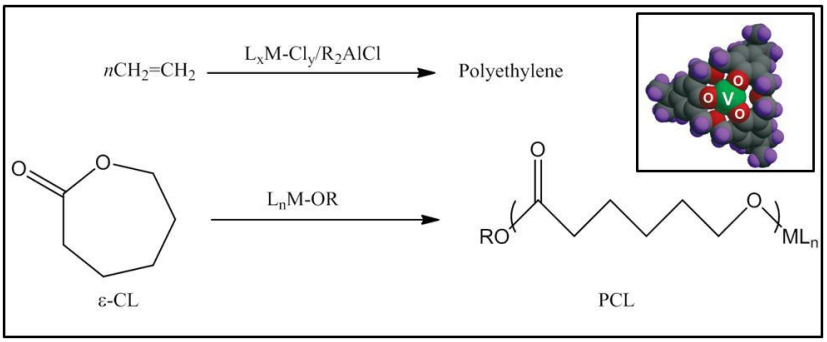

Figure 1. Typical polymerization processes investigated herein. Inset shows one of our recently reported V-based catalysts.

Available to calixarenes	Benefit
Easily prepared	Multigram quantities
Readily functionalized	Solubility control
Chirality incorporation	Enantio-discrimination
Cavity	Substrate recognition
Multiple binding sites	Cooperative effects
Can fix to supports	Heterogeneous catalysis

Table 1. Properties and catalytic benefits of calixarenes.

Polymerisation of α-olefins

Building on earlier work from Matt *et al*., [8] Taoufik, Bonnamour and coworkers have investigated the use of titanacalix[4]arenes for ethylene polymerization. In particular, reaction of 1,3-dialkoxycalix[4]arene$(OH)_2(OR)_2$ with $[TiCl_4(THF)_2]$ afforded, following work-up, high yields of complexes of the type $[TiCl_2$(p-*tert*-butylcalix[4]arene$(O)_2(OR)_2]$ (R = Me **1**, Et **2**, *n*Pr **3**, *i*Bu **4**). The molecular structure of **4** is shown in Figure 2. The French groups also prepared a number of titanium complexes of depleted 1,2- and 1,3-calix[4]arenes (see **5** and **6**, Chart 1 top) in high yield via the use of $[TiCl_4]$; the depleted calixarenes are available via the use of diethyldiphosphate ester precursors using p-*tert*-butylcalix[4]arene$(OH)_4$/$ClP(O)(OEt)_2$/Et_3N followed by reductive cleavage in the presence of K/NH_3. The structures of **5** (two signals for the methylene protons; $^2J_{HH}$ 16.7 Hz) and **6** (six sets of signals for the methylene protons with ratio 1:2:2:1:1:1; $^2J_{HH}$ 13.0 – 15.6 Hz) were confirmed by their ^{1}H NMR spectra and 2D NOESY experiments.

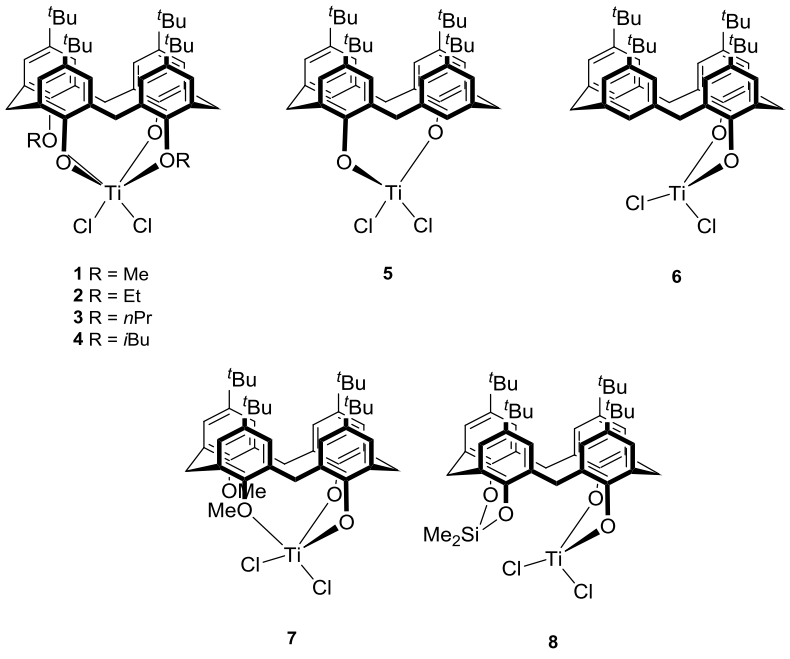

Chart 1.Titanacalix[4]arenes **1** – **8**.

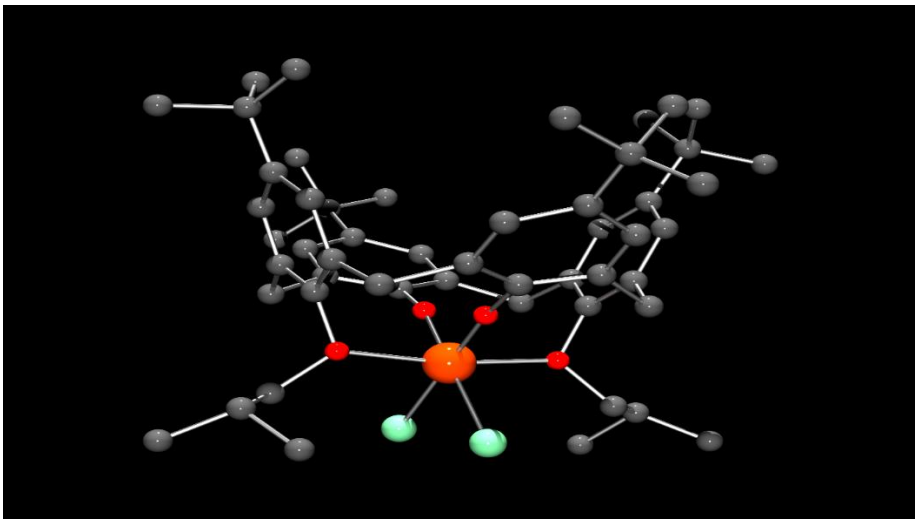

Figure 2. Molecular structure of titanacalix[4]arene **2**.

A 1,2-dimethoxycalix[4]arene$(O)_2(OMe)_2$ titanium complex **7** (Chart 1, bottom left) was also reported for which ^{1}H NMR spectroscopic data was consistent with only one of the methoxy groups coordinating to the Ti centre (δ 4.09 *versus* 1.67 ppm). For the silyloxide complex **8** (Chart 1, bottom right), the calix[4]arene binds in bi-dentate fashion to both the metal centre and the Si centre. [9]

These titanacalixarene complexes were screened for their potential in ethylene polymerization using MAO as co-catalyst under 30 bar and at 50 ^{o}C, and despite only low to moderate activity ($\leqslant$ 770 g/mmolTi.h) being achieved; a number of structure/activity relationships were identified. In particular, the catalyst systems can be divided into two families: the distal titanacalixarenes **1** – **5** afforded UHMWPE (M_n 2.3 x 10^6 to 3.2 x 10^6 gmol^{-1}), whereas the proximal titanacalixarenes **6** and **8** afforded HDPE (M_n 1.4 x 10^6 (**6**) and 1.7 x 10^6 (**8**) gmol^{-1}). The best catalytic activities were observed for the proximal systems, with **6**/MAO achieving the highest activity (350 g/mmolTi.h). By contrast, much lower activities were observed for the distal systems **1** - **4** ($\leqslant$21 g/mmolTi.h), suggesting that within this series variation of the alkoxy groups at the lower rim had little influence on either the resultant polymer properties or on the observed catalytic activity. Comparison of **5** (1,3-)

versus **6** (1,2-) revealed that **6** was almost twice as active as **5**, which may well reflect the distorted tetrahedral/square planar (O – Ti – O 106.4 ^{o}) *versus* angles which are more associated with distorted octahedral (O – Ti – O 96.2 ^{o}) coordination environments in **6** and **5** **(**the metal remains 4-coordinate here**)** , respectively. The coordinatively unsaturated catalytic species generated from **5** led to the production of higher molecular weight polyethylene than that produced when using **1 - 4** whose octahedral geometries were not favourably predisposed towards the binding of ethylene. Overall, it appeared that increasing the number of proximal substituents was detrimental in terms of catalytic activity or put another way, increasing the number of ether oxygens present led to decreased productivity.

Given that complex **6**/MAO outperformed the other systems in the initial screening, it was subjected to a more detailed study in which the temperature and the pressure were varied. The activity was found to peak (770 g/mmolTi.h) at 70 ^{o}C and 30 bar, whilst further elevating the temperature led to drastically reduced activities most likely reflecting the thermal instability of the system. For all runs, the M_w/M_n values remained below 6. Despite the melting points of the polymers remaining relatively constant (133.9 – 136.6 ^{o}C), the temperature did influence the molecular weight (M_n), such that the highest M_n was observed at 60 ^{o}C and the lowest at 80 ^{o}C. As expected, increases in pressure (from 5 to 30 bar) led to both increased activity and amount of polymer formed.

Using the depleted 1,3-calix[4]arene compounds utilized in the above titanium studies, [9] we prepared a number of vanadyl and vanadium imido complexes (see **9** – **12**, Chart 2). The synthesis involved reaction of the depleted 1,3-calix[4]arene$H_2(OH)_2$ with vanadium reagents in the form of (oxo/imido) trialkoxides, and the reaction proceeded with loss of alcohol; complex **12** was formed as a minor hydrolysis product. [10] Dimeric **9** possesses a pseudo 2-fold symmetry axis, and contains two 4-coordinate distorted tetrahedral vanadyl centres. The structures of **10** and **11** resemble that of **9** with approximate 2*mm* symmetry. In the case of **12**,

a V_4O_4 network (ladder-like) links the two calix[4]arene units. Each 'central' V centre is 5-coordinate adopting a square pyramidal geometry (vanadyl group apical), whilst the 'outer' vanadyl centres are better described as adopting trigonal bipyramidal geometries.

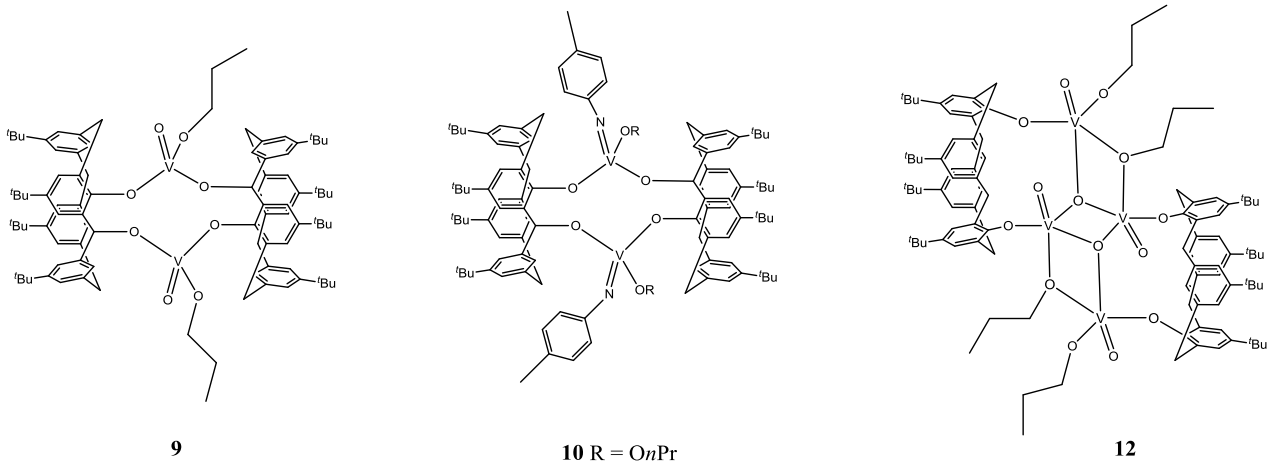

9 **10** R = O*n*Pr
11 R = O*t*Bu **12**

Chart 2. Vanadium complexes **9** – **12** bearing 1,3-depleted calix[4]arenes.

Screening using either DMAC (dimethylaluminium chloride) or MDAC (methylaluminium dichloride) as co-catalyst in the presence of ETA (ethyl trichloroacetate) as re-activator was conducted. Both **9** and **10** exhibited similar behaviour with either of the co-catalysts and were highly active at 80 ^{o}C (with DMAC $\leqslant$ 15,800 g/mmol.h.bar; with MDAC $\leqslant$ 10,500 g/mmol.h.bar). In the case of the *tert*-butoxide **11**, the thermal stability was somewhat reduced such that the highest observed activity occurred at 40 ^{o}C (DMAC) or 60 ^{o}C (MDAC). The situation for complex **12** was more akin to that observed for **9** and **10** with enhanced thermal stability leading to high activity at elevated temperatures (80 ^{o}C). In the presence of either co-catalyst, the systems employing **12**, closely followed by those of **9**, tended to outperform the other systems screened. The polymer morphology appeared to change at around 60 ^{o}C from a thick jelly-like solid to a fine white powder. In the context of other vanadyl calixarene complexes screened under similar conditions, activities for **9** – **12** were similar to those observed for the multi-metallic calix[4]arene complexes {[V(O)p-*tert*-

butylcalix[4]arene$(O)_4]_2$(μ-2,6-CH_2pyCH_2)} and {[VO(O*n*Pr)]$_2$(μ-O)p-*tert*-butylcalix[4]arene$(O)_2(OMe)_2$}. [5] However, they were inferior to those observed for the oxacalix[3]arene complexes [V(X)p-*tert*-butylhexahomooxacalix[3]arene$(O)_3$] (X = O, 92,500 g/mmol.h.bar at 80 ^oC; Np-tolyl, 129,400 g/mmol.h.bar at 80 ^oC), but surpassed those observed for the monomeric methylether-p-*tert*-butylcalix[4]arene complexes [V(X)calix[4]arene$(OMe)(O)_3$] (X = O, 1,400 g/mmol.h.bar at 45 ^oC; Np-tolyl, 1,500 g/mmol.h.bar at 45 ^oC) and the dimeric complex [Vcalix[4]arene$(O)_4(NCMe)]_2$ (1,300 g/mmol.h.bar at 45 ^oC). [5]

In collaboration with Equistar Chemicals, complex **12** was screened under more industrially relevant conditions. Runs were conducted using either TEA (triethylaluminium) or DEAC (diethylaluminium chloride) as co-catalyst at 220 ^oC and 29 bar ethylene in the presence of H_2. However, under such conditions, unfortunately no polymeric material was isolated. Also as part of this collaboration, complexes **9** and **10** were supported on silica. Screening under slurry conditions resulted in the formation of polyethylene, albeit with low activity ($\leqslant$ 30 g/mmol.h). [11]

Given the positive impact that resulted on the catalytic activity of a number of group V based calix[*n*]arene systems from the changing of the methylene (-CH_2-) bridges to dimethyleneoxa (-CH_2OCH_2-) bridges, [5] we decided to investigate the influence that changing to thia (-S-), sulfinyl (-SO-) or sulfonyl (-SO_2-) bridges might impart.

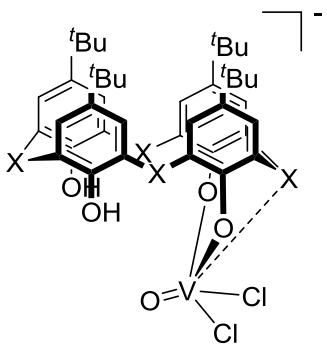

13 X = S
14 X = SO
15 X = SO_2

Chart 3. Vanadyl anions bearing thia (**13**), sulfinyl (**14**) or sulfonyl (**15**) calix[4]arenes; cation is PPh_4.

The synthetic methodology employed by Limberg for the thia complex **13** (addition of $PPh_4[VO_2Cl_2]$ to the parent calixarene in THF) was extended by us to complexes **14** and **15** (see Chart 3).

In **14**, the coordination sphere at the distorted octahedral vanadium centre involves binding to an oxygen of one of the sulfinyl bridges. This bond is quite long (2.191 Å), which may reflect its position *trans* to the vanadyl group. The macrocycle in **14** retains the cone conformation. For **15**, the binding at the metal is similar to that observed in **14**, whereas the conformation adopted by the calix is very different, namely an ′up-up-up-down′ conformation – the differing conformations are illustrated in Figure 3.

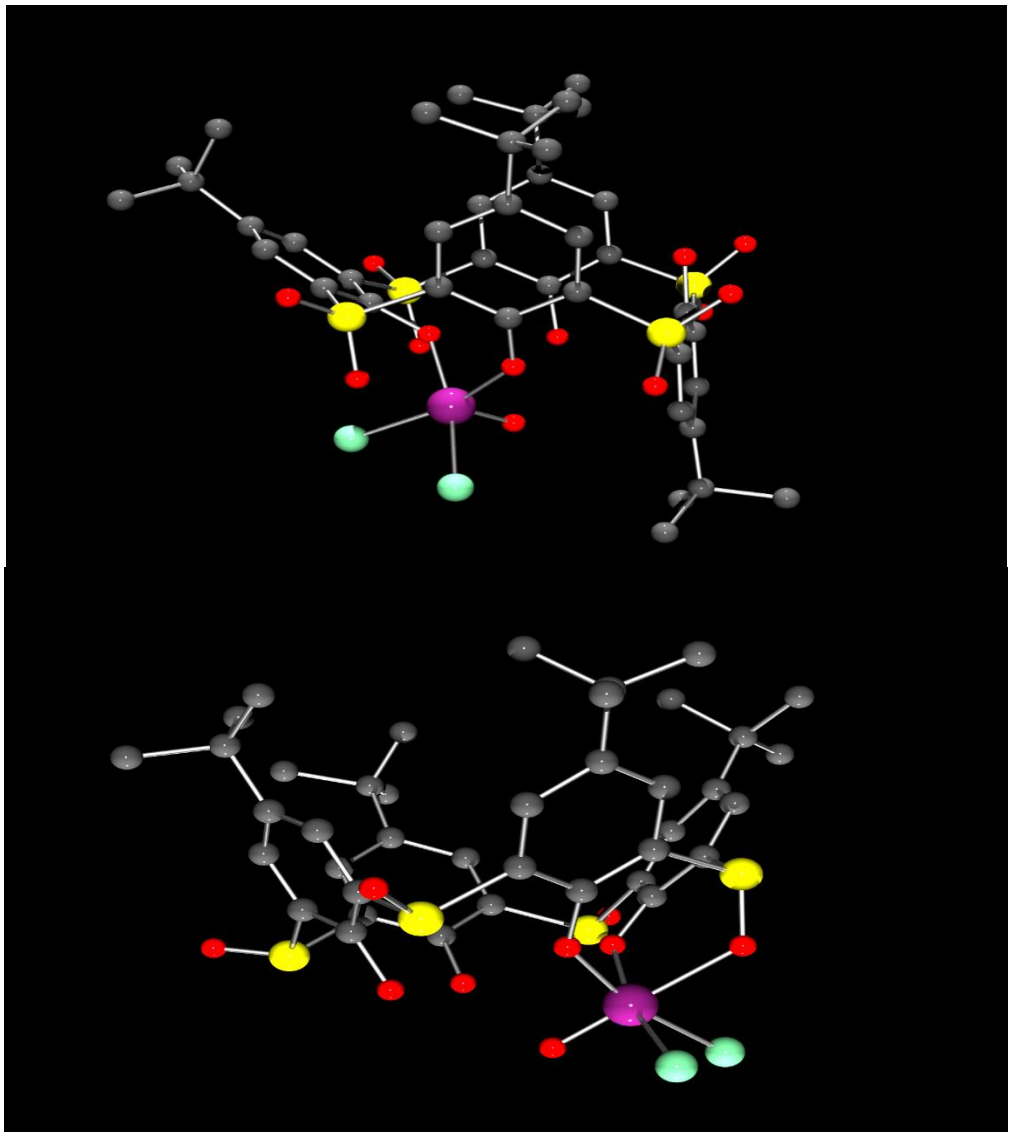

Figure 3. Molecular structures of top **14**, and bottom **15**.

All three complexes were then screened for their ability to polymerize ethylene using either DMAC or MDAC as co-catalyst and ETA as re-activator; results were compared against [V(O)p-*tert*-butylhexahomooxacalix[3]arene(O)$_3$]. Optimized conditions using the thia complex **13**/DMAC were found to be an [Al]:[V] ratio of 6000:1 at a temperature of 60 ^{o}C, which afforded an activity of 13,800 g/mmol.h.bar (and for **13**/MADC, 26,200 g/mmol.h.bar). Surprisingly, the system **14**/DMAC was poor (< 1000 g/mmol.h.bar), whereas **14**/MDAC exhibited enhanced thermal stability and high activity (37,400 g/mmol.h.bar at 80 ^{o}C). In the case of **15**/DMAC, increasing the [Al]:[V] ratio led to a steady increase in activity (eg, for

8000:1, activity = 25,100 g/mmol.h.bar), whilst for **15**/MDAC, an [Al]:[V] ratio of 6000:1 at 60 ^{o}C afforded an activity of 44,000 g/mmol.h.bar. Under such conditions, the order of activity **15** > [V(O)p-*tert*-butylhexahomooxacalix[3]arene(O)$_3$] > **14** > **13** was observed, which suggested that the presence of the donor oxygens in the bridge was indeed beneficial here. High molecular weight, linear polyethylene was obtained in all cases, for which melting points were in the range 138 – 140 ^{o}C. Molecular weights were substantially reduced at the higher temperatures, although the PDIs were narrower (eg 4.3 at 40 ^{o}C *versus* 2.7 at 80 ^{o}C for **15**).

The improved performances when using MADC *versus* DMAC were thought to arise due to the nature of the active species which is presumed to contain multiple V – Cl – Al bridges. Such bridges are likely to be more readily formed using MADC given the multiple chlorides available. Preparative reactions of the co-catalysts (5 equivalents) with these vanadium complexes revealed that the initial reaction took place at the phenolic groups, and V(IV) species were formed. The initial interaction between organoaluminium reagents and the phenolic groups is unsurprising, and is consistent with the vanadium-aluminium-phenoxide cluster proposed by Gambarotta. [12] In a number vanadyl systems, we have seen a correlation between V(IV) concentration and observed catalytic activity. [13]

Vigalok *et al* have prepared a new family of tetradentate *N,O*-type compounds in the form of amine disubstituted calix[4]arenes. The procedure worked well when using CuOTf as the catalyst and *i*PrOH as solvent and allowed access to pyrazole, piperidine, morpholine, pyrrolidine, 1-phenyl piperazine and (R)-2-methyl pyrrolidine derivatives. In the case of the pyrazole compound, further reaction with [$TiCl_4$] in refluxing toluene afforded [$TiCl_2$(p-*tert*-butylcalix[4]arene(O)$_2$(NR$_2$)$_2$)] (**16**, R = $C_3H_3N_2$, see Chart 4) in 75 % yield. The ^{15}N NMR of 16 exhibited two doublets at δ 279.5 and 208.0 ppm, which are somewhat different to those observed for the parent ligand set, *viz* 298.6 and 211.8 ppm. A single crystal X-ray analysis confirmed the pyrazole ring binding mode at the metal (see Figure 4).

This compound was screened for its ability to polymerize 1-hexene, both when activated by $B(C_6F_5)_3$ or in the presence of MAO (500 equivalents) in the absence of any solvent at ambient temperature. Only in the presence of MAO was reasonable activity (15 g/mmol.h) observed affording high molecular (186 KDa) atactic (as determined by ^{13}C NMR spectroscopy) polymer, and with low polydispersity (1.44). It also proved possible to use **16**/MAO to polymerize styrene, both neat and in toluene, affording in each case syndiotactic polymer. [14]

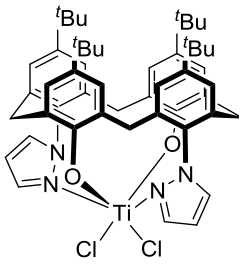

16

Chart 4. Complex $[TiCl_2(p\text{-}tert\text{-butylcalix[4]arene}(O)_2(NR_2)_2)]$ (**16**, R = $C_3H_3N_2$).

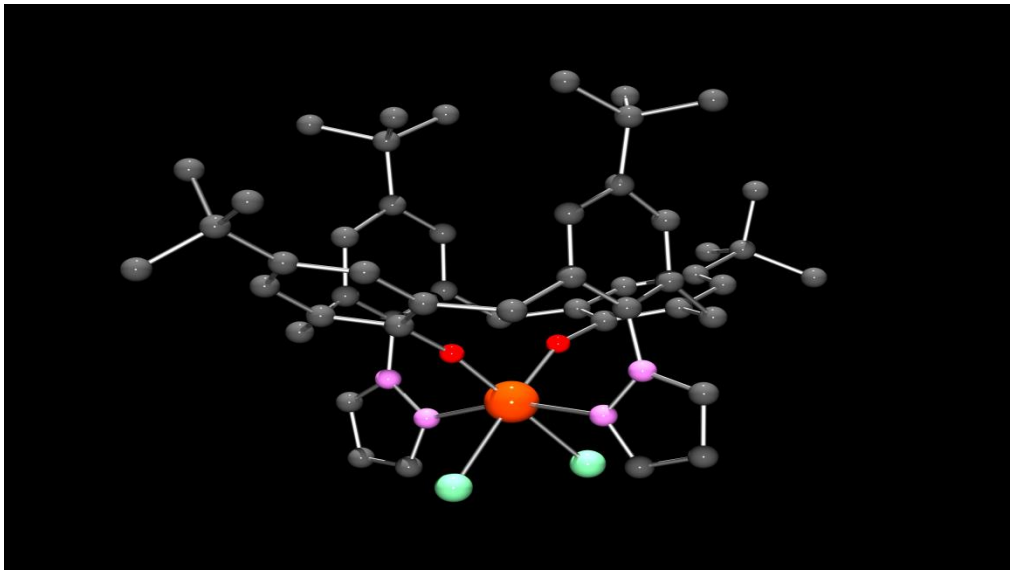

Figure 4. Molecular structure of [$TiCl_2$(p-*tert*-butylcalix[4]arene$(O)_2(NR_2)_2$)] (**16**, R = $C_3H_3N_2$).

In collaboration with the Mitsui Chemical Inc. (Chiba, Japan) and Borealis Polymers (Porvoo, Finland), we have investigated the homo- and co- (with either propylene or 1-hexene) polymerization of ethylene using catalytic systems employing vanadyl calix[6]arenes. The complexes **17**, **18** and **19** (Chart 5) are prepared in one of two ways, firstly, in the case of **17** (and **18**), by adding *in-situ* generated [$LiVO(OtBu)_4$] to the parent p-*tert*-butylcalix[6]arene$(OH)_6$ or for **19**, reversing the addition such that [$VOCl_3$] was added to the lithiated calix[6]arene. The resulting structures are very different with **17** adopting what can best be described as a 'calixarene sandwich', in which the filling is two 5-coordinate vanadium centres linked via their vanadyl oxygen atoms by a lithium cation. This 4-coordinate lithium is further coordinated by a solvent molecule (acetonitrile) and a protonated calixarene oxygen atom. A further *exo* lithium cation balances the overall charge.

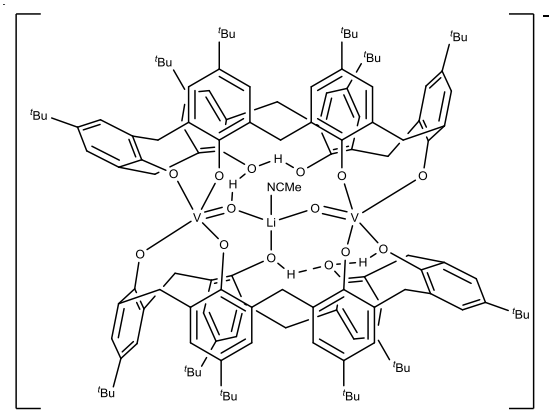

17

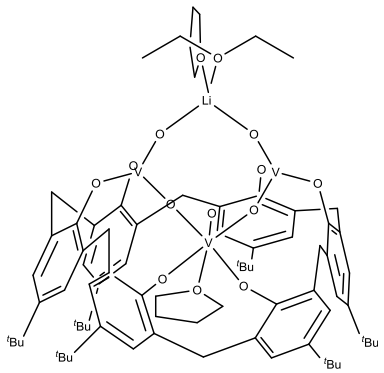

19

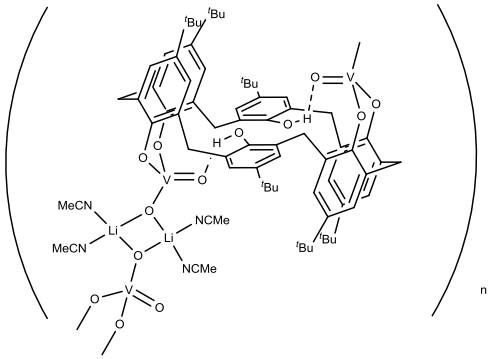

18.2MeCN

Chart 5. Vanadyl calix[6]arene complexes **17** – **19**.

On occasion, this reaction can also result in the formation of a secondary minor product (*ca*. 10 %) of formula $\{[(VO_2)_2$(p-*tert*-butylcalix[6]arene$(O)_4(OH)_2)(Li(MeCN)_2)_2]\cdot 2MeCN\}_n$ **18**·2MeCN. The structure of this product (**18**) is a 1D polymeric chain comprised of linkages formed by Li_2O_2 diamond-shaped units and the chair p-*tert*-butylcalix[6]arene$(O)_4(OH)_2$ ligand, the former lithiated linkages bridge the calixarene bound metal centres. Various views of this structure are presented in Figure 5.

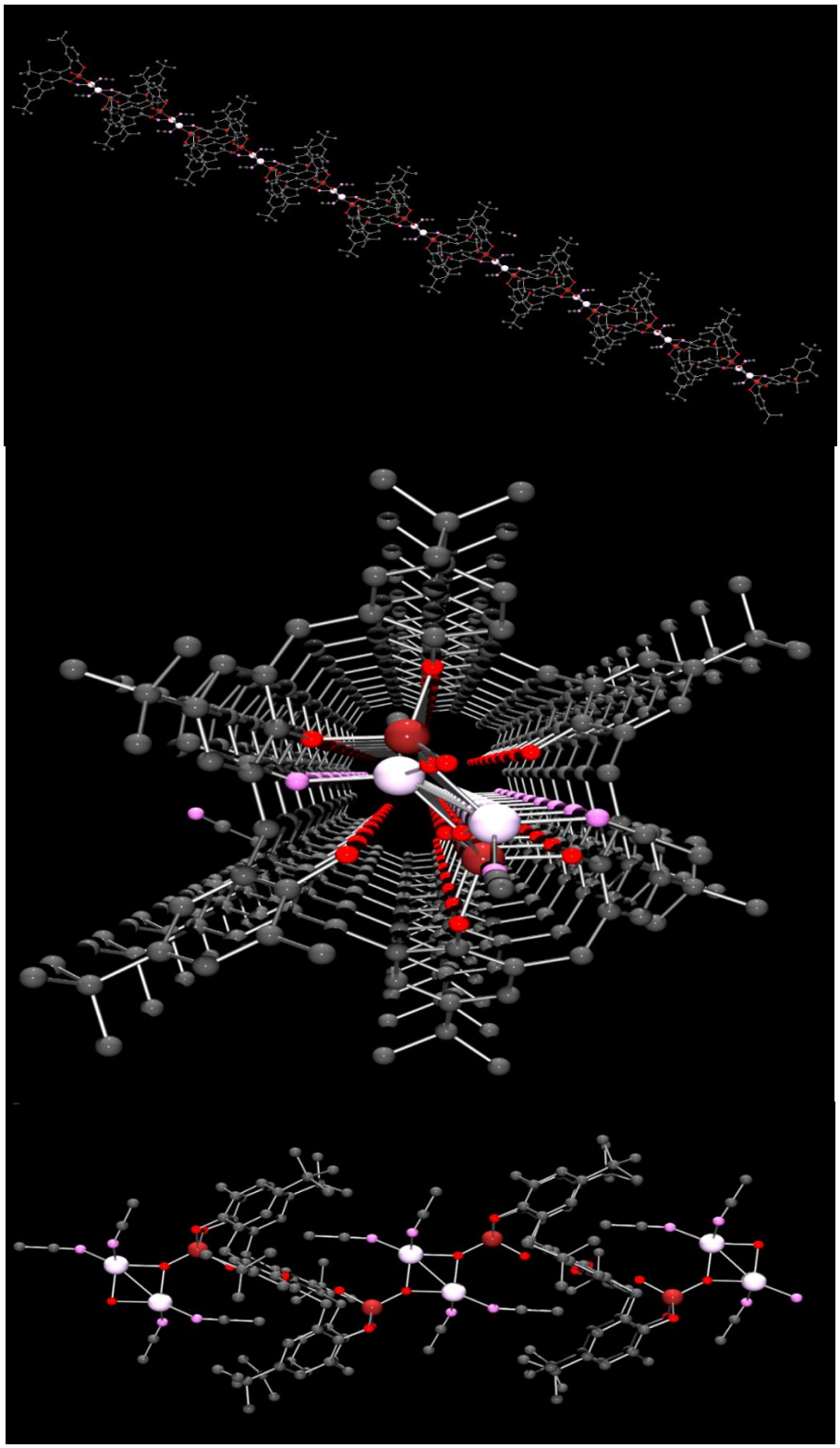

Figure 5. Three views of the molecular structure of {[$(VO_2)_2$(p-*tert*-butylcalix[6]arene$(O)_4(OH)_2$)(Li$(MeCN)_2)_2$]·2MeCN}$_n$ **18**·2MeCN; top, the 1D chain; middle end on; bottom, a snap shot of the chain.

The reverse addition affords a trinuclear motif (**19**) in which two tetrahedral vanadyl centres are linked via an octahedral vanadyl centre, and also via a lithium cation bound by two solvent molecules. This motif is attached to a single calix[6]arene which adopts a 'down, down, down, down, out, out' conformation. The two synthetic routes are highlighted in Chart 6.

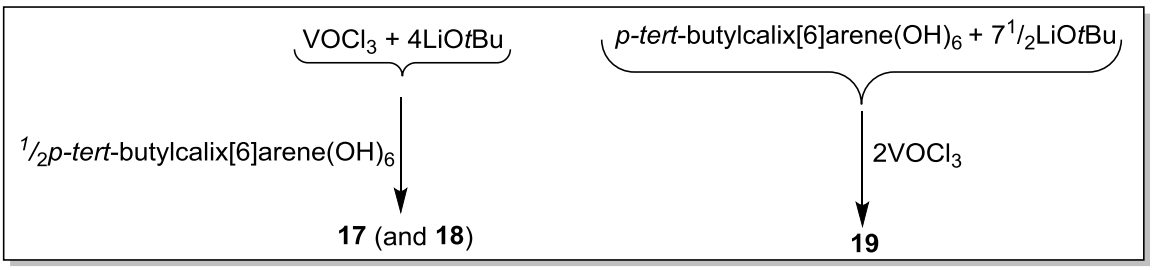

Chart 6. Synthetic routes to **17**- **19**.

Preliminary ethylene polymerization screening of **17**/MADC/ETA revealed that the activity peaked (13,800 g/mmol.h.bar) at 60 ^{o}C for an [Al]:[V] ratio of 4000:1. A lower [Al]:[V] ratio or use of DMAC as co-catalyst afforded inferior results.

Complex **17** was refluxed in toluene for 12 h with pre-treated (heated *in vacuo* at 350 ^{o}C for 48 h) silica, and any unreacted complex was removed by further washing. Use of XPS on the supported sample **S17** was consistent with 0.24 % vanadium in the bulk sample. This supported sample was subjected to ethylene polymerization screening (heterogeneous conditions) using either TIBA (triisobutylaluminium) or EADC (ethylaluminium dichloride) as co-catalyst (both in the presence of ETA), however monomer uptake was the result of solvent saturation only, *ie* the systems were inactive. For the co-polymerization of ethylene with 1-hexene, use of the supported system **S17** proved to be more successful. The activity (3050 g/mmol.h.bar) peaked at 80 ^{o}C using EADC/ETA; use of TIBA was less fruitful. Given

these co-polymerizations results, the observed inactivity for the homo-polymerization of ethylene is somewhat surprising.

Using a parallel pressure reactor (8 reaction vessels with monomer feed lines), **17**/DMAC/ETA was found to be highly active (202,480 g/mmol.h) at 0.8MPa and high temperature (80 ^{o}C). However, these higher temperatures led to decreased polymer molecular weight (M_w), for example 640,700 (50 ^{o}C) *cf* 30,200 (110 ^{o}C). Similar use of DEAC generally led to lower activities, the exception being at 140 ^{o}C (3000 g/mmolV.h *cf* 1,160 g/mmolV.h for DMAC).

Results (activities) for **19**/DMAC/ETA were much lower than those when using **17**, although use of **19** afforded UHMWPE at 50 ^{o}C. Results for **17** and **19** were compared with the system [VO(OEt)Cl_2]/DMAC (or DEAC)/ETA as a benchmark. The benchmark systems were inactive at 140 ^{o}C, whilst at other temperatures, it tended to outperform **19**, but was inferior to **17** when using DMAC or comparable to **17** when using DEAC. Also, in general, the polymer molecular weights (M_w) obtained using the benchmark systems were lower than those observed when employing either **17** or **19**. ^{13}C NMR spectroscopic analysis of the polymers indicated that there was no branching present.

System **17**/DMAC/ETA was also found to be highly active (107,080 g/mmolV.h) for the co-polymerization of ethylene/propylene at 50 ^{o}C, whilst the active of **19**/DMAC/ETA was 18,780 g/mmolV.h, with 8.2 and 7.4 mol% C3 incorporation, respectively. Under the same conditions, the benchmark system afforded an activity of 156,240 g/mmolV.h with 10.0 mol% C3 incorporation. For **17**, use of DEAC instead of DMAC led to lower activities and molecular weights (M_w), though it did outperform the benchmark system in terms of activity and C3 incorporation. Use of Me_3Al a co-catalyst afforded far lower activities (600 g/mmolV.h). [15]

Given the promising results above achieved with the p-*tert*-butylcalix[6]arene$(OH)_6$, we extended our studies to related systems based on p-*tert*-butylcalix[8]arene$(OH)_8$ (see **20** – **22**, Chart 7). Similar synthetic strategies were employed, namely complex **20** was prepared by adding *in-situ* generated [$NaVO(O$*t*$Bu)_4$] to the parent p-*tert*-butylcalix[6]arene$(OH)_6$. In the resultant salt [$Na(NCMe)_5$][$(VO)_2$p-*tert*-butylcalix[8]arene$(O)_7(OH)$ **20**, the anion contains a macrocycle adopting a saddle-shaped conformation, whilst the two pseudo octahedral vanadium centres are linked by asymmetric aryloxide bridges. The structure of **20** is related to the structure of a complex reported by Limberg (phosphonium salt) and proposed by Pedersen (ammonium or alkali metal salt). [16] It proved possible to prepare an alkali-metal free complex [$(VO)_4$p-*tert*-butylcalix[8]arene$(O)_8(\mu^3$-O)] (**21**) via the interaction of [$VO(O$*t*$Bu)_3$] with p-*tert*-butylcalix[8]arene$(OH)_8$ in the presence of adventitious oxygen. In **21**, the macrocycle adopts a shallow, saddled-shaped conformation and is bound by four 5-ccordinate, square pyramidal vanadyl centres. The core structure of vanadium/oxygen atoms forms a ladder-like arrangement. Complex **22** was obtained in a similar manner to **19**, whereby the lithiated calixarene was treated with [$VOCl_3$] (two equivalents). Following work-up, the complex [$(VO_2)_2Li_6$(p-*tert*-butylcalix[8]arene$(O)_8)(THF)_2(O$*t*$Bu)_2(Et_2O)_2$] (**22**) was isolated, which given it lies on a 2-fold axis, only half is unique. The central core is comprised of a lantern shape for which Li_2O_2 diamonds form the top and bottom and four 8-membered panels form the sides. The lithiums of this lantern bind to calixarene oxygens and to the oxygens of the four vanadium centres. Two views of the molecular structure of **22** are presented in Figure 6.

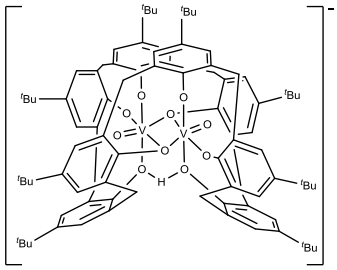

20

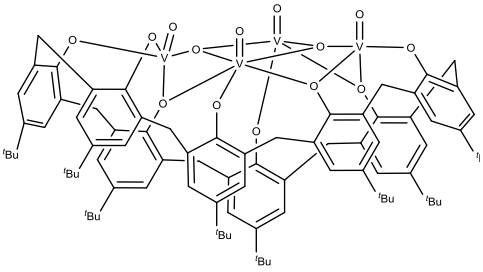

21

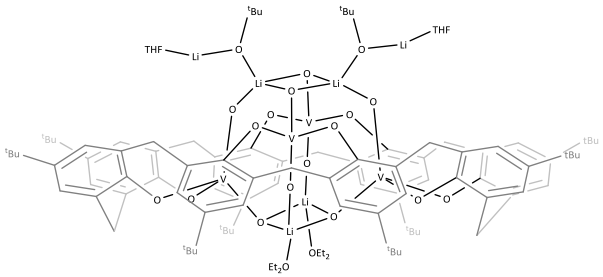

22

Chart 7. Vanadium complexes **20** – **22** bearing calix[8]arenes.

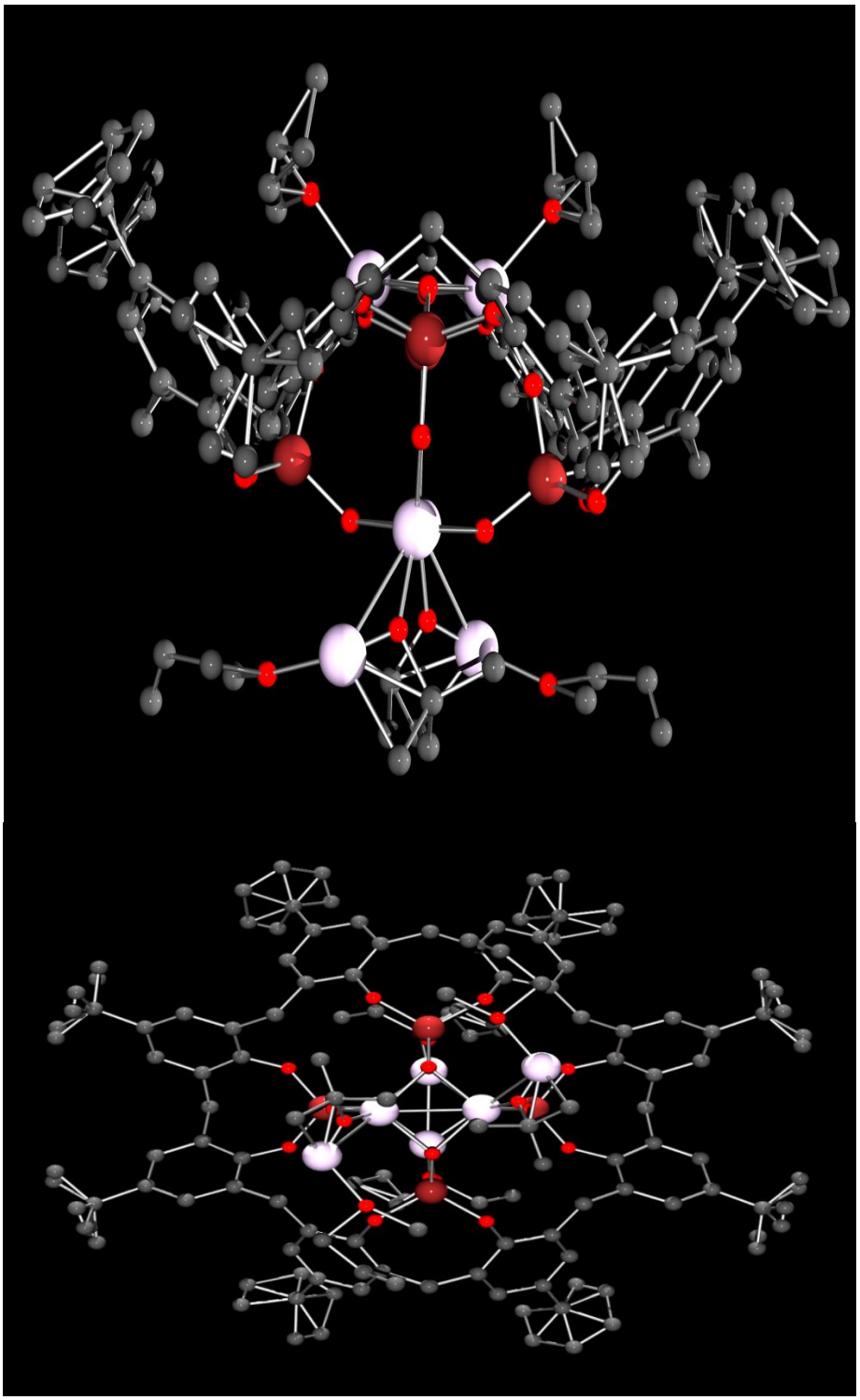

Figure 6. Two views of the molecular structure of **22**.

In collaboration with Mitsui Chemical Inc., complexes **20** - **22** have been screened for their potential to polymerize ethylene in the presence of a variety of co-catalysts including DMAC, DEAC, Me_3Al, Et_3Al or DMAO (dried MAO) with and without ETA. Systems employing Me_3Al, Et_3Al or DMAO did not function catalytically, whilst for the other co-catalysts, it

proved necessary to add ETA to achieve high activity. Indeed, the trend was for higher observed activity with increased [ETA]:[Al] ratio. For complex **20**/DMAC/ETA ([Al]:[V] = 20,000) at 80 ^{o}C, an activity of 163,000 g/mmolV.h; the system was inactive at 140 ^{o}C. Molecular weights also dropped off rapidly as the temperature increased. In the case of **19**/DEAC/ETA, the system was not as thermally stable and peaked at 50 ^{o}C (73,000 g/mmolV.h). Whilst the PDI for the DMAC system (*ca*. 2.0) suggested a single species was active at higher temperatures, that for the DEAC system was far broader (>25) suggestive of multiple catalytic centres. In the case of **21**/DMAC/ETA, reasonable activity (101,000 g/mmolV.h) was observed at 50 ^{o}C, but this dropped off dramatically (*ca*. 8200 g/mmolV.h) at 110 ^{o}C. Results using **21**/DEAC/ETA were considerably worse (by about an order of magnitude). Results (activity trends) for **22**/DEAC/ETA were similar to those of **21**, though the molecular weights (M_w) were generally higher than those observed for **20** and **21**. The use of DEAC was again inferior to the use of DMAC, although interestingly, the activity observed at 110 ^{o}C was as low as 920 g/mmolV.h, yet at 140 ^{o}C this had increased to over 7500 g/mmolV.h. When this is considered also in terms of the broadening of the PDI at the higher temperature, it suggests that new active species are generated and responsible for the activity hike. [17] In most cases, observed activities were lower than those obtained using the benchmark complex [VO(OEt)Cl_2], although it is noteworthy that the complex **22** with either co-catalyst (and ETA) outperformed the benchmark systems. Furthermore, under many of the conditions employed, higher molecular weight polymers were obtained than using the benchmark system. The high molecular weight polymers formed showed no evidence of branching.

As a quick comparison guide, data for the runs of selected ethylene polymerization catalysts systems described above are presented in Table 2.

Table 2. Selected ethylene polymerization results.†

System	Conditions	Activity (g/mmolM.h)	M_w or M_n	M_w/M_n	Reference
3/MAO	50 °C, 30 bar, 2 h	21	3,200,000 (M_n)	2.9	9
5/MAO	50 °C, 30 bar, 2 h	185	2,600,000 (M_n)	3.3	9
6/MAO	70 °C, 30 bar, 2 h	770	1,000,000 (M_n)	4.9	9
9/DMAC/ETA	80 °C, [Al]:[V] 2000, 1 bar, 15 min.	15,800	-	-	10
11/DMAC/ETA	40 °C, [Al]:[V] 2000, 1 bar, 15 min.	10,200	-	-	10
13/DMAC/ETA	60 °C, [Al]:[V] 6,000, 1 bar, 15 min.	13,800	-	-	11
14/MDAC/ETA	80 °C, [Al]:[V] 6,000, 1 bar, 15 min.	37,400	-	-	11
15/MDAC/ETA	60 °C, [Al]:[V] 6,000, 1 bar, 15 min.	44,000	-	-	11
17/DMAC/ETA	80 °C, [Al]:[V]:[ETA] 20,000:1:20,000, 8 bar	202,480	105,200 (*Mw*)	2.6	15
19/DEAC/ETA	50 °C, [Al]:[V]:[ETA] 20,000:1:20,000, 8 bar	52,650	1,544,400 (M_w)	2.5	15
20/DMAC/ETA	80 °C, [Al]:[V]:[ETA] 20,000:1:20,000, 8 bar	163,000	133,000 (M_w)	2.4	17
21/DMAC/ETA	50 °C, [Al]:[V]:[ETA] 20,000:1:20,000, 8 bar	101,000	752,000 (M_w)	6.4	17
22/DMAC/ETA	50 °C, [Al]:[V]:[ETA] 20,000:1:20,000, 8 bar	104,000	945,000 (M_w)	5.0	17

† MAO = methylaluminoxane; DMAC = dimethylaluminium chloride; DEAC = diethylaluminium chloride; MDAC = dimethylaluminium chloride; ETA = ethyl trichloroacetate.

Ring opening polymerisation of cyclic esters

Given the ready availability of the depleted 1,3-calix[4]arenes from our ethylene polymerization studies discussed above, [10] we examined their ε-caprolactone ROP capability. For the systems screened (see Chart 2), it was found that little or no polymer was obtained at temperatures below 80 °C. However at 80 °C, the vanadyl complex **9** exhibited good conversion (94 %) and control (M_w/M_n 1.1) over 72 h affording low molecular weight

polymers. The essentially isostructural organoimido complexes **10** and **11** performed much poorer with % conversions of 46 % and 20 % respectively. The poor performance of **11** was attributed to the increased steric bulk at the metal.

The –S-, -SO- and –SO_2- bridged calix[4]arene vanadyl complexes **13** – **15** (Chart 3) were also screened for their catalytic potential in the ROP of ε-caprolactone in the presence of BnOH. However, under the conditions [CL]:[V] = 400:1 over the temperature range 25 to 80 ^{o}C and using 0 to 5 equivalents of BnOH in toluene, the systems were inactive. [11]

Zinc is a favoured metal centre for ROP catalyst systems, [18] and given this, we have studied a number of p-*tert*-butylcalix[4]arene$(OH)_2(OnPr)_2$ (**23** – **25**, Chart 8) and p-*tert*-butylhexahomocalix[3]arene$(OH)_3$ derived zinc systems (**26** and **27**, Chart 9) as potential ROP catalysts for ε-caprolactone and *rac*-lactide. The complexes were prepared by direct interaction of the diarylzinc reagent with the parent calixarene (for **23** and **26**), reaction with $\{Zn[N(SiMe_3)_2]_2\}$ (for **24**) or treatment of the parent calix[4]arene with NaH (two equivalents), followed by addition of $[ZnCl_2]$ and $NaN(SiMe_3)_2$. Those systems containing a C_6F_5 – Zn moiety required high temperatures (in a variety of solvents) to achieve activity for the ROP of either ε-caprolactone and *rac*-lactide, and this barrier was thought to be due to the difficulties in generating the required catalytic alkoxide in the presence of BnOH. Polymer molecular weights were far lower than expected, consistent with substantial transesterification occurring. In the case of the oxacalix[3]arene system **26**, the situation was further complicated by degradation to more complicated species such as **27** (see Chart 9 and Figure 7) in which a number of the oxacalix[3]arene rings had been cleaved. [19]

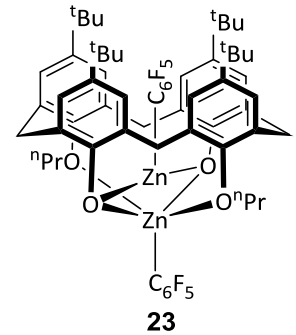

23

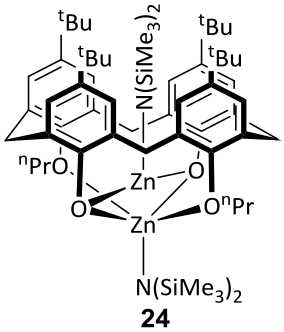

24

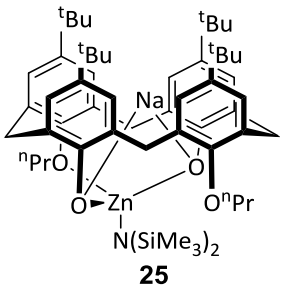

25

Chart 8. Zinc complexes **23** – **25** bearing p-*tert*-butylcalix[4]arene$(O)_2(OnPr)_2$

Of the systems shown in Chart 8, only the silylamide complex **24** was found to be capable of the ROP of ε-caprolactone at ambient temperature, with 65% conversion over 4h and molecular weights close to the theoretical values. If the $(Me_3Si)_2N$ – Zn grouping in the calixarene cavity is replaced by a sodium cation, then the resulting system **25** is no longer active under the conditions employed for **24**. All the zinc systems, when operating at high temperatures, were still well controlled with PDIs typically in the range 1.06 – 1.48.

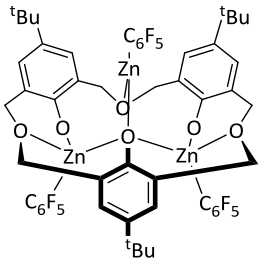

26

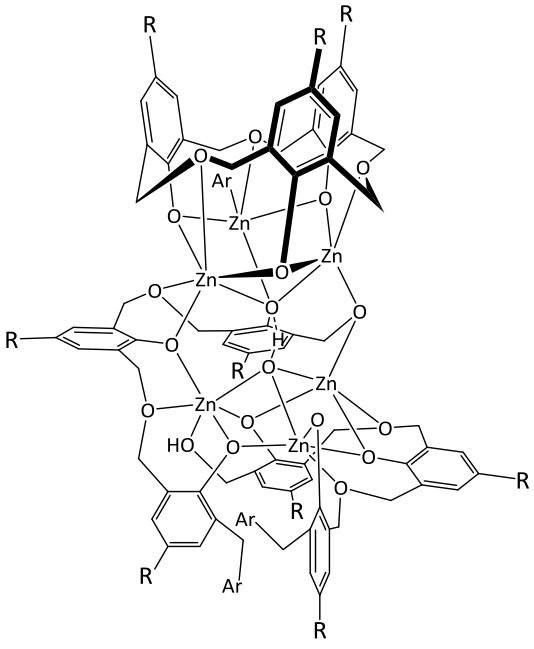

27 (Ar = C_6F_5; R = *t*Bu)

Chart 9. Pentafluorophenyl zinc complexes **26** and **27** bearing ligands derived from oxacalix[3]arene.

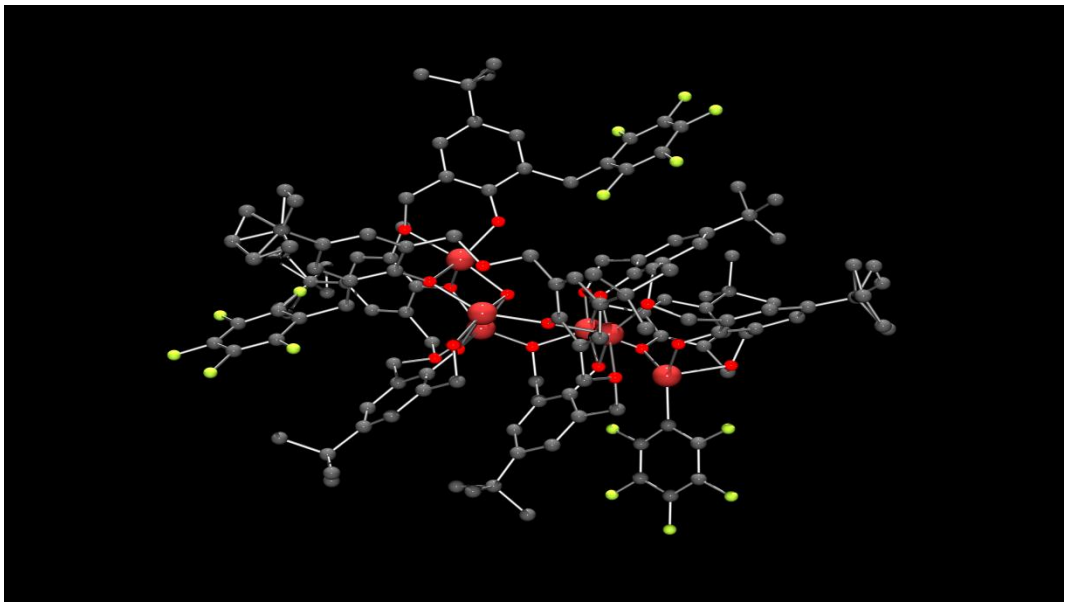

Figure 7. The molecular structure of **27**.

We are also interested in developing group VI metal catalysts for ROP, [20] and with this in mind have investigated the reaction of $[W(eg)_3]$ (eg = 1,2-ethanediolato) with calix[6 and 8]arene$(OH)_{6,8}$. This allowed access to a family of tungstocalix[6 and 8]arenes – see **28** – **32**, Chart 10. For p-*tert*-butylcalix[6]arene$(OH)_6$, these included an oxo-bridged complex $\{[W(eg)_2](\mu\text{-}O)$p-*tert*-butylcalix[6]arene$(O)_6\}$ (**28**) formed when using $\leqslant$2 equivalents of $[W(eg)_3]$, whilst use of excess $[W(eg)_3]$ and in the presence of molecular sieves, the complex $\{[W(eg)_2]$p-*tert*-butylcalix[6]arene$(O)_4(OH)_2\}$ (**29**) was isolated. In the solid state structure of **28**, each tungsten centre is bound by a 1,2-eg ligand, and adopts a distorted octahedral geometry. A near linear (W-O-W 164.7(6) ^{o}) oxo bridge links the two tungsten centres. The calix[6]arene conformation is best described as an enlarged cup (see Figure 8).

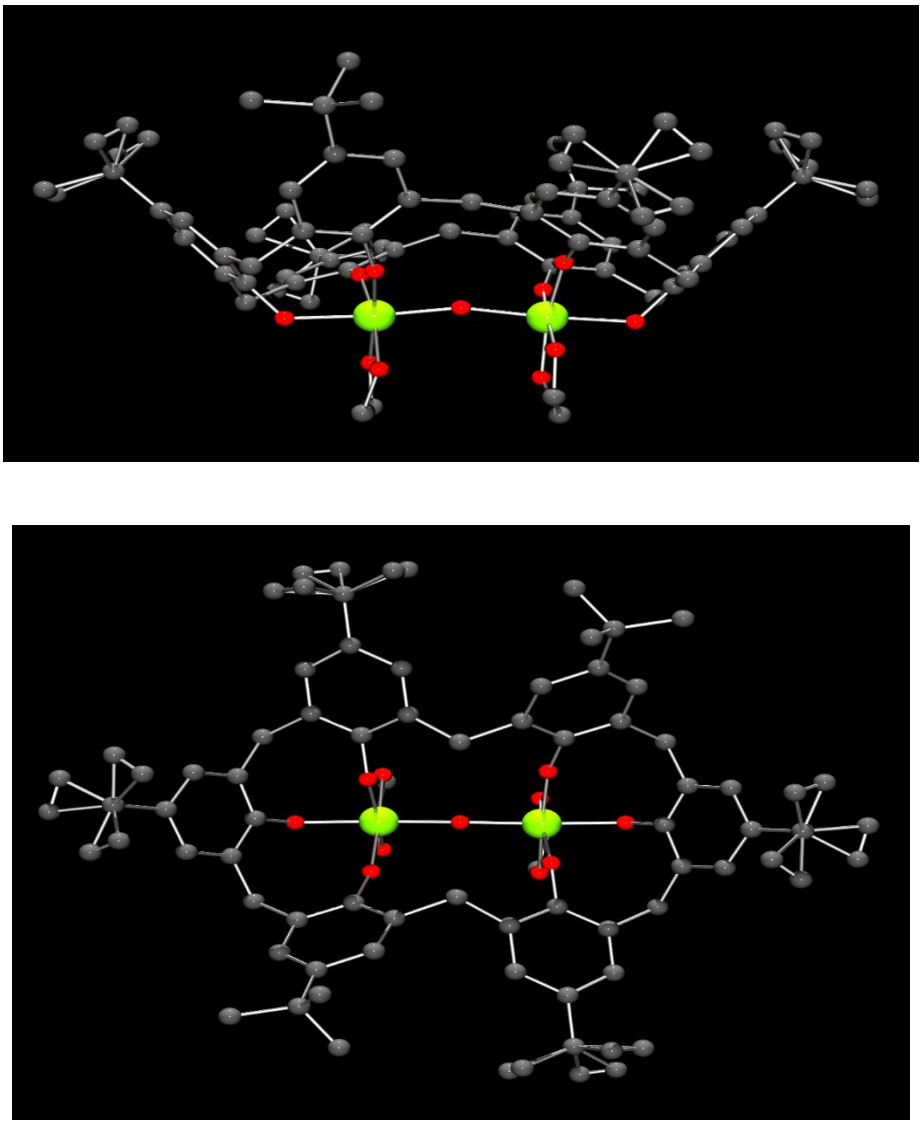

Figure 8. Two views of the molecular structure of **28**.

A similar strategy using p-*tert*-butylcalix[8]arene$(OH)_8$ led, in the case of ⩽2 equivalents of $[W(eg)_3]$, to the complex $\{[W(eg)_2]$p-*tert*-butylcalix[8]arene$(O)_8\}$ (**30**), whilst with four equivalents, a mixture of two isomers **31**, namely $\{1,2\text{-}[W(eg)_2]$p-*tert*-butylcalix[8]arene$(O)_4(OH)_4\}$ and $\{1,3\text{-}[W(eg)_2]$p-*tert*-butylcalix[8]arene$(O)_4(OH)_4\}$, was isolated. In the structure of **30**, the calix[8]arene twists to accommodate the two bulky distorted octahedral $W(eg)_2$ fragments. For the isomer mixture **31**, the major isomer comprises two tungsten centres bound to adjacent calixarene phenolate oxygens, whereas in the minor isomer, a phenolic group separates the pairs of phenolate oxygens that bind to the

tungsten centres. Extension to the dioxacalix[6]arene p-*tert*-butyltetrahomodioxacalix[6]arene$(OH)_6$ afforded the complex {[$WO(eg)_2]_2$p-*tert*-butyltetrahomodioxacalix[6]arene$(O)_4(OH)_2$} (**32**), in which each of the dimethyleneoxa bridges is bound to a tungsten(VI) oxo centre. Further binding by two adjacent calixarene phenoxides results in *fac* arrangements at each tungsten centre. The conformation of the calixarene is folded, which results in tungsten centres residing at the opposite corners of a rectangle. These tungsten complexes were screened for their potential to ring open polymerize ε-caprolactone under a variety of conditions and for comparative purposes, the known calix[4]arene complex {[W(eg)]p-*tert*-butylcalix[4]arene$(O)_4$} was also screened. [21] Optimization of the catalytic conditions using {[$W(eg)_2$]p-*tert*-butylcalix[6]arene$(O)_4(OH)_2$} (**29**) activated with BnOH revealed that activity was only achieved at temperatures in excess of 100 ^oC over prolonged periods (> 12h). Temperatures above 110 ^oC led to a reduction in both conversion rates and average molecular weights (M_n). The system exhibited characteristics typical of a living process. The molecular weight could be increased by increasing the [Cl] to [W] ratio, for example on going from 100:1 to 1000:1 the molecular weight (M_n) increased from 18.82 x 10^3 to 52.83 x 10^3. Using these optimized conditions, it was found that the other calix[6]arene containing systems were active, however there was no improvement in activity by employing the dimethyleneoxa bridges, which contrasts with the observations noted during α-olefin polymerization when using group V based systems. [4] The resulting polymers were capped by a benzyl ester group and a hydroxyl group consistent with the insertion of a benzyloxy group into the CL.

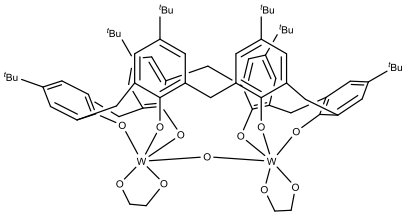

28

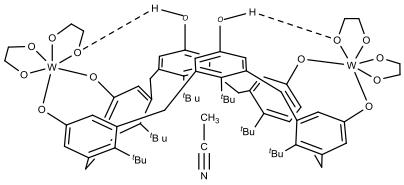

29

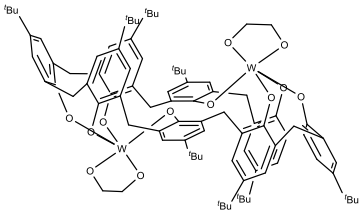

30

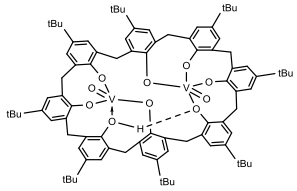

31 (1,2-)

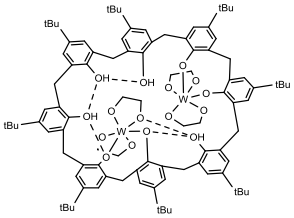

31 (1,3-)

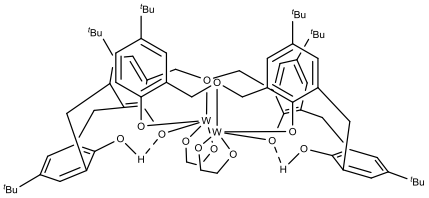

32

Chart 10. Calix[6 and 8]arene complexes **28 - 32** bearing W(eg) fragments.

The complex {[W(eg)]p-*tert*-butylcalix[4]arene$(O)_4$} was found to be less active the calix[6]arene-based systems. Interestingly, the calix[8]arene-based systems **30** and **31** were found to be inactive, which was tentatively assigned to unfavourably increased conformational flexibility associated with the larger macrocycle which in some way hindered the ROP process. [22]

The best performing systems we have observed to-date involve the use of calix[4]arenes bearing *n*-propyl groups at the lower rim and bound by *n*-butyl magnesium. Two complexes were prepared (**33** and **34**, Chart 11, for molecular structure of **34**, see Figure 9), the first of which, prepared in *ca*. 30 % yield via the interaction of *n*BuMgBr (two equivalents) with 1,3-dipropoxy-p-*tert*-butylcalix[4]arene$(O)_2(OLi)_2$ in THF at 0 ^oC, was a heterobimetallic complex, namely

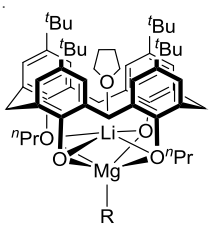

33 R = *n*Bu

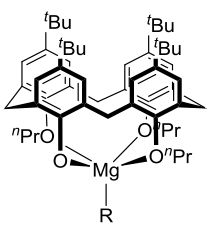

34 R = *n*Bu

Chart 11. Organomagnesium complexes **33** and **34**.

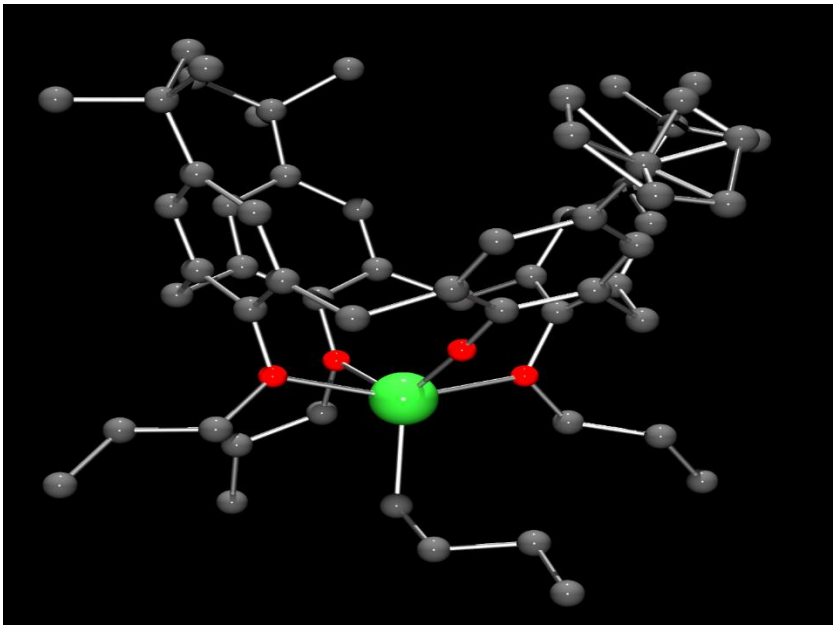

Figure 9. Molecular structure of magnesium complex **34**.

[Li(THF)Mg(*n*Bu)(1,3-dipropoxy-p-*tert*-butylcalix[4]arene(O)$_4$)] (**33**) in which the lithium resides in the cavity. The presence of the lithium forces the calixarene to adopt an elliptical conformation; the magnesium and lithium centres are 2.670(5) Å apart. The second complex was prepared from p-*tert*-butylcalix[4]arene(O*i*Pr)$_3$(OH), which on interaction with *n*Bu$_2$Mg (one equivalent) in THF at 0 ^{o}C afforded the complex [Mg(*n*Bu)(p-*tert*-butylcalix[4]arene(O*i*Pr)$_3$(O))] (**34**) in 50 % isolated yield. Both these complexes were found to be highly active for the ROP of *rac*-lactide. Indeed, complex **34** can be described as being exceptionally active in either toluene or THF (less active in CH_2Cl_2), taking only 3 minutes to achieve >90 % conversion; best conversions were observed on addition of BnOH, *i*PrOH or *t*BuOH but not MeOH. Indeed, in THF, the addition of MeOH was found to deactivate the system. However, when using BnOH in either THF or toluene, the alcohol acts a as chain transfer agent allowing for good chain length control for the polymer such that the systems can be describe as immortal.

For complex **33**/BnOH in THF, quenching the 'polymerization' procedure with excess methanol resulted only in the isolation of methyl-(RS)-lactate, and so the preferred method was to use **33**/MeOH in CH_2Cl_2, quenching with a drop of hydrochloric acid. Although this solvent system afforded the highest activity (in contrast to complex **34**), the polymer produced had nearly twice the expected molecular weight, which resulted from the formation of a magnesium chloride (reaction of CH_2Cl_2 with Mg – *n*Bu) which was incapable of ROP and so led to an enhanced monomer:catalyst ratio.

The stereochemistry of the resultant PLA was assigned by using 2D J-resolved ^{1}H NMR spectroscopy, whereby the 1D spectrum of the resultant PLA is separated out with coupling constant appearing on the y-axis. By projecting onto the x-axis, all coupling is removed and assignments can be made using literature values. [23] Such a method is advantageous in that it is fully automated and there is no need to manually input information as is the case for homonuclear decoupled spectroscopy. In the case of **33** and **34**, both afforded atactic (Pr = 0.41 – 0.49) PLA in CH_2Cl_2. Interestingly, in THF, complex **34** exhibited high selectivity for heterotactic PLA (Pr = 0.78 – 0.85), but in toluene isotactic PLA (Pr = 0.30 – 0.36), making catalytic system unique in that it is both a highly active, immortal and stereoselective. [24]

In a preliminary communication, McIntosh and coworkers have reported a titanium p-*tert*-butylcalix[8]arene complex [Ti_4(*p*-*tert*-butylcalix[8]arene)(O*n*Pr)$_8$(THF)$_2$] (**35**) in which the conformation of the macrocycle is best described as adopting a double cone (see Chart 12 and Figure 10). Both terminal and bridging *n*-propoxide ligation is present, the latter linking the two Ti_2 units. The preparation involved reacting four equivalents of [Ti(O*n*Pr)$_4$] with the parent calix[8]arene in THF affording the complex in 37 % isolated yield. The complex has been screened for its ability to ROP *rac*-lactide. At 130 ^{o}C over 16 h, polymer was isolated which possessed M_w with a max of $^m/_z$ 1956, and with O*n*Pr end groups. The lower than indicated M_w values and the presence of a family of peaks separated by half the monomer

unit were suggestive of the presence of transesterification and cyclic esters. The % conversion was not reported, however further studies are in-progress. [25]

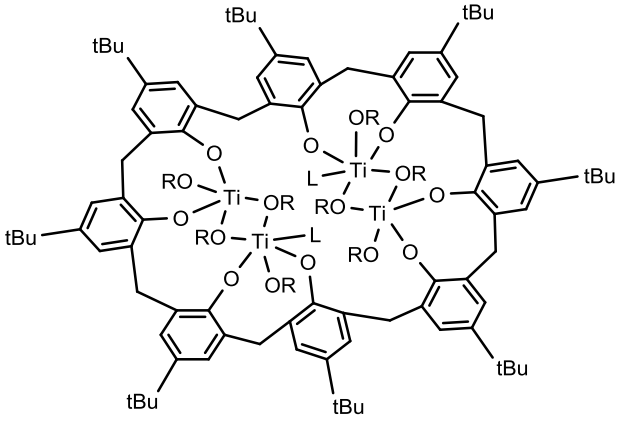

35 R = *n*Pr, L = THF

Chart 12. Titanium complex **35**.

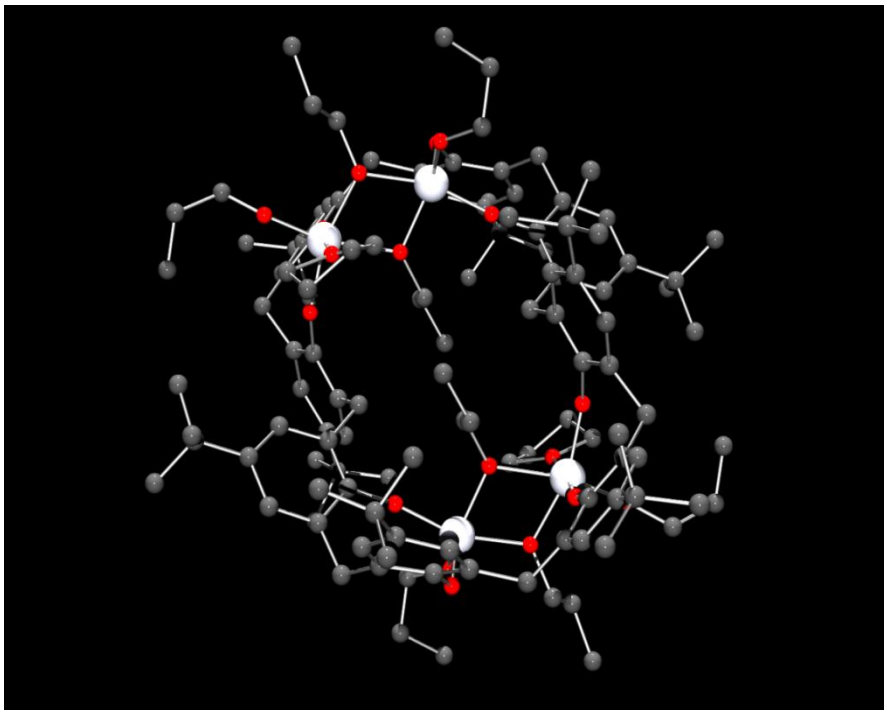

Figure 10. Molecular structure of **35**.

As a quick comparison guide, data for the runs of selected ring opening polymerization catalysts systems described above are presented in Table 3.

Table 3. Selected ring opening polymerization results.†

System	Conditions	Conversion (%)	M_n	M_w/M_n	Reference
9/ε-CL/BnOH	Toluene, [CL]:[V];[BnOH] 400:1:5, 80 °C, 72 h	94	3,100	1.1	10
10/ε-CL/BnOH	Toluene, [CL]:[V];[BnOH] 400:1:5, 80 °C, 72 h	46	3,900	1.1	10
11/ε-CL/BnOH	Toluene, [CL]:[V]:[BnOH] 400:1:5, 80 °C, 72 h	20	5,400	1.3	10
13-15/ε-CL/±BnOH	Toluene, [CL]:[V] 400, 0 – 5 equiv. BnOH, 25-80 °C.	0	-	-	11
24/ε-CL/BnOH	Toluene, [Zn]:[BnOH] 100, 20 °C, 4 h	65	1190	1.27	19
29/ε-CL/BnOH	Toluene, [CL]:[W]:[BnOH] 400:1:1, 110 °C, 48 h	99.3	40,830	1.08	22
33/*rac*-LA/MeOH	CH_2Cl_2, [Mg]:[MeOH] 100, 20 °C, 1 h	55	15,400	1.22	24
34/*rac*-LA/BnOH	THF, [Mg]:[BnOH] 100, 20 °C, 3 min	92	14,800	1.25	24
35/*rac*-LA	[Ti]:[LA] 100, 130 °C, 16 h	-	-	-	25

† ε-CL = ε-caprolactone, *rac*-LA = *rac*-lactide, BnOH = benzyl alcohol.

Conclusion

As for any ligand set, it is the combination with and coordination sphere created at the requisite metal centre/central element that dictates the catalytic ability of the system. What calixarenes bring to the table is their versatile functionalization which allows for tuneable steric and/or electronic properties, which in turn can be used to manipulate physical

properties such as solubility. When employing larger calix[*n*]arenes, there can be a play-off between beneficial cooperative effects achieved by binding metals in close proximity *versus* blocking of access to the catalytic centre by unfavourable conformational flexibility. An underexplored area of metallocalix[*n*]arene chemistry is their use as nanopots/nanoreactors, [26] the catalytic pockets of which allow for internal '*endo*' metal/substrate binding, and have the potential to achieve unusual selectivities. Such studies are currently underway in our laboratory.

Acknowledgements

I would like to thank all of my collaborators for their efforts. The EPSRC are thanked for an overseas travel grant, and Northwest University (Xi'an) is thanked for financial support.

References

[1] (a) S. J. Dalgarno, P. K. Thallapally, L. J. Barbour and J. L. Atwood, *Chem. Soc. Rev*. **2007**, 32, 236-245. (b) B. Mokhtari, K. Pourabdollah and N. Dallali, J. Radioanal. Nucl. Chem. **2011**, 287, 921-934. (c) S. B. Nimse and T. Kim, *Chem. Soc. Rev*. **2013**, 42, 366-386.

[2] C. Redshaw, *Coord. Chem. Rev*. **2003**, 244, 45-70.

[3] D. Homden and C. Redshaw, *Chem. Rev*. **2008**, 108, 5086-5130.

[4] (a) C. Redshaw, D. Homden, D. L. Hughes, J. A. Wright and M. R. J. Elsegood, *Dalton Trans*. **2009**, 1231-1242. (b) C. Redshaw, M. Rowan, D. M. Homden, M. R. J. Elsegood, T. Yamato and C. Pérez-Casas, *Chem. Eur. J*. **2007**, 13, 10129–10139.

[5] C. Redshaw, M. A. Rowan, L. Warford, D. M. Homden, A. Arbaoui, M. R. J. Elsegood, S. H. Dale, T. Yamato, C. Pérez-Casas, S. Matsui and S. Matsuura, *Chem. Eur. J*. **2007**, 13, 1090-1107.

[6] (a) C. A. Wheaton, P. G. Hayes and B. J. Ireland, *Dalton Trans*. **2009**, 4832-4846. (b) A. Arbaoui and C. Redshaw, *Polym. Chem.* **2010**, 1, 801-826. (c) C. Redshaw. *Dalton Trans*. **2010**, 39, 5595-5604. (d) A. Sauer, A. Kapelski, C. Fliedel, S. Dagorne, M. Kol and J. Okuda, *Dalton Trans*. **2013**, 42, 9007-9023. (e) S. Dagorne, M. Normand, E. Kirillov and J. –F. Carpentier, *Coord. Chem. Rev*. **2013**, *257*, 1869-1886.

[7] Metal Alkoxides. Ed. Jacob Zabicky, Publisher Patai, Y. Li, K.-Q. Zhao, C. Redshaw, A. Y. Nuñez, B. A. M. Ortega, S. Memon and T. A. Hanna, **2014**.

[8] M. Frediani, M. Sémeril, A. Comucci, L. Bettucci, P. Frediani, L. Rosi, D. Matt, L. Toupet, W. Kaminsky, *Macromol. Chem. Phys.* **2007**, 208, 938-945.

[9] J. Espinas, U. Darbost, J. Pelletier, E. Jeanneau, C. Duchamp, F. Bayard, O. Boyron, J.-P. Broyer, J. Thivolle-Cazat, J.-M. Basset, M. Taoufik and I. Bonnamour, *Eur. J. Inorg. Chem*. **2010**, 1349-1359.

[10] L. Clowes, C. Redshaw, and D. L. Hughes. *Inorg. Chem*. **2011**, 50, 7838-7845.

[11] C. Redshaw, L. Clowes, D. L. Hughes, M. R. J. Elsegood and T. Yamato, *Organometallics*, **2011**, 30, 5620-5624.

[12] S. Gambarotta, *Coord. Chem. Rev*. **2003**, 237, 229-243.

[13] (a) I. E. Soshnikov, N. V. Semikolenova, A. A. Shubin, K. P. Bryliakov, V. A. Zakharov, C. Redshaw and E. P. Talsi, *Organometallics* **2009**, 28, 6714-6720. (b) I. E. Soshnikov, N. V. Semikolenova, K. P. Bryliakov, A. A. Shubin, V. A. Zakharov, C. Redshaw and E. P. Talsi, *Macromol Chem. Phys*. **2009**, 210, 542-548. (c) . E. Soshnikov, N. V. Semikolenova, K. P. Bryliakov, V. A. Zakharov, C. Redshaw and E. P. Talsi, *J. Mol. Cat. A. Chem*. **2009**, 303, 23-29.

[14] V. Rawat, K. Press, I. Goldberg and A. Vigalok, *Org. Biomol. Chem.*, **2015**, 13, 11189-11193.

[15] C. Redshaw, M. Walton, K. Michiue, Y. Chao, A. Walton, P. Elo, V. Sumerin, C. Jiang and M. R. J. Elsegood, *Dalton Trans.* **2015**, 44, 12292-12303.

[16] (a) E. Hoppe, C. Limberg, B. Ziemer, *Inorg. Chem*. **2006**, 45, 8308-8317. (b) G. E. Hofmeister, F. E. Hahn, S. F. Pedersen, *J. Am. Chem. Soc*. **1989**, 111, 2318-2319. (c) G. E.

Hofmeister, E. Alvarado, J. A. Leary, D. I. Yoon, S. F. Pedersen, *J. Am. Chem. Soc*. **1990**, 112, 8843-8851.

[17] C. Redshaw, M. J. Walton, D. S. Lee, C. Jiang, and M. R. J. Elsegood and K. Michiue, *Chem. Eur. J*. **2015**, 21, 5199-5210.

[18] See Y. Sarazin and J. –F. Carpentier, *Chem. Rev*. **2015**, 115, 3564–3614 and references therein.

[19] M. J. Walton, S. J. Lancaster, J. A. Wright, M. R. J. Elsegood and C. Redshaw, *Dalton Trans*. **2014**, 43, 18001-18809.

[20] (a) W. Yang, Q. -K. Zhao, C. Redshaw, and M. R. J. Elsegood, *Dalton Trans*, **2015**, 44, 13133-13140. (b) Y. Al-Khafaji, T. J. Prior, M. R. J. Elsegood and C. Redshaw, *Catalysts* **2015**, 5, 1928-1947.

[21] A. Lehtonen and R. Sillanpää, *Polyhedron*, **1998**, 17, 3327-3330.

[22] Y. Li, K.-Q. Zhao, C. Feng, M. R. J. Elsegood, T. J. Prior, X. Sun, and C. Redshaw, *Dalton Trans*. **2014**, 43, 13612-13619.

[23] T. K. Sen, A. Mukherjee, A. Modak, S. K. Mandel and D. Koley, *Dalton Trans*. **2013**, 42, 1893-1904.

[24] M. J. Walton, S. J. Lancaster and C. Redshaw, *Chem. Cat. Chem.* **2014**, 6, 1892-1898.

[25] J. D. Ryan, K. J. Gagnon, S. J. Teat and R. D. McIntosh, *Chem. Commun*. **2016**, Advanced article. **DOI:** 10.1039/C6CC00478D

[26] E. Guzmán-Percástegui, D. J. Hendández and I. Castillo, *Chem. Commun*. **2016**, 52, 3111-3114.

Biography

Carl Redshaw is Chair of Inorganic Materials at the University of Hull. He received his Ph. D at Newcastle University, was a Welch Fellow at the University of Texas (Austin) and a postdoc with the late Sir G. Wilkinson at Imperial College (IC). Following 2 years at Durham University and a further stint at IC, he was awarded a Leverhulme Special Research Fellowship at moved to UEA as Lecturer, Senior Lecturer and Reader. He was appointed Professor of Inorganic Materials at Hull in 2012. He has been Visiting Professor at the Shanghai Institute of Organic Chemistry (SIOC) and the Institute of Chemistry (ICCAS), Beijing and Guest Professor at Sichuan Normal University in Chengdu. He is currently Guest Professor at Northwest University in Xi'an. Research interests include calixarene chemistry, polymerisation catalysis and the use of metal-based anti-cancer agents.